RSC Advances

PAPER

View Article Online
View Journal | View Issue

Cite this: *RSC Adv.*, 2021, **11**, 35687

High ionic conduction, toughness and self-healing poly(ionic liquid)-based electrolytes enabled by synergy between flexible units and counteranions†

Fu Jie Yang, ‡*[a] Qing Feng Liu,‡[a] Xiao Bing Wu,[a] Yu Yi He,[a] Xu Gang Shu[a] and Jin Huang *[b]

Polymer electrolytes offer great potential for emerging wearable electronics. However, the development of a polymer electrolyte that has high ionic conductivity, stretchability and security simultaneously is still a considerable challenge. Herein, we reported an effective approach for fabricating high-performance poly(ionic liquids) (PILs) copolymer (denoted as **PIL-BA**) electrolytes by the interaction between flexible units (butyl acrylate) and counteranions. The introduction of butyl acrylate units and bis(trifluoromethane-sulfonyl)imide ($TFSI^-$) counteranions can significantly enhance the mobility of polymer chains, resulting in the effective improvement of ion transport, toughness and self-healability. As a result, the **PIL-BA** copolymer-based electrolytes containing $TFSI^-$ counterions achieved the highest ionic conductivity of 2.71 ± 0.17 mS cm^{-1}, 1129% of that of a PIL homopolymer electrolyte containing Cl^- counterions. Moreover, the **PIL-BA** copolymer-based electrolytes also exhibit ultrahigh tensile strain of 1762% and good self-healable capability. Such multifunctional polymer electrolytes can potentially be applied for safe and stable wearable electronics.

Received 12th June 2021
Accepted 14th October 2021

DOI: 10.1039/d1ra04553a

rsc.li/rsc-advances

Introduction

With the rapid development of wearable electronic devices, flexible solid-state batteries possessing high energy density have captured both academic and industrial attention in recent years.[1,2] As one of the key components in flexible batteries, solid polymer electrolytes (SPEs) are inevitably subjected to external deformations like stretching, folding and bending in practical use, which may easily lead to damage of the SPEs that hinders the transportation of ions between the cathode and the anode, and severely deteriorates the battery performance.[3,4] Assuming that the SPEs can be endowed with self-healing function, it will automatically repair cracks and damage. This will largely improve the reliability of flexible solid-state batteries.

Based on the above motivation, quite a few self-healable SPEs containing the covalent or non-covalent bonds such as disulfide bonds,[5,6] hydrogen bonds,[7–9] and ionic bonds,[10–12] have been identified in the past decades. Among several different classes, polymerized ionic liquids or so-called poly(ionic liquid)s (PILs) formed from ionic liquid (IL) monomers are a promising candidate for intrinsic self-healing SPEs with the reversible ionic interactions between the charged polymer backbones and counter-ions.[13–15] Moreover, PILs have been applied in some electrochemical devices like sensors, dye-sensitized solar cells, and lithium ion batteries, because they combine the mechanical durability of the polymer with the electrochemical properties of the ionic liquids.[16–19] However, the ionic conductivities of PILs are relatively lower than that of the corresponding ILs,[20–22] leading to the deterioration of the whole performance of assembled devices. In the past few years, it was found that in PILs, ion transport and self-repairing capability are largely dependent on the mobility of polymer chains.[8,23] Various efficient measures like plasticizing,[24] interpenetrating,[25] and copolymerizing[26] were utilized to decrease the glass-transition temperature (T_g) of polymers for promoting the movement of polymer chains. Among them, in the reported strategy of copolymerization, the polymer backbones of SPEs were chemically modified by the effective functional groups on the molecular level. In this way, the SPEs were obtained with high ionic conductivity, good electrochemical stability and excellent mechanical performance while improving the mobility of polymer chains.[27] It has been reported that the T_g values of polymers can be significantly decreased by grafting the ester groups into the main chains of the polymer through copolymerization.[28–30] For instance, Guo *et al.* reported PIL copolymers containing ethyl acrylate units with excellent healing properties at 55 °C due to the higher mobility of the counteranions and the polymer chains.[30] However, the prepared PIL copolymer as

[a]*College Chemistry and Chemical Engineering, Zhongkai University of Agriculture and Engineering, Guangzhou 510275, P. R. China. E-mail: yangfujie580@163.com*

[b]*College of Pharmacy, Guangxi Medical University, Nanning 530021, P. R. China. E-mail: huangjin@mailbox.gxnu.edu.cn*

† Electronic supplementary information (ESI) available. See DOI: 10.1039/d1ra04553a

‡ Fu Jie Yang and Qing Feng Liu contributed equally to this work.

polymer electrolyte shows an low ionic conductivity (1.6×10^{-7} S cm^{-1}) at 25 °C, which is far from the require of batteries. Most recently, Cai and coworkers have prepared a PIL-based quasi-solid state copolymer electrolyte for lithium–sulfur batteries by polymerization of butyl acrylate (BA) with IL monomer and crosslinked with poly(ethylene glycol)diacrylate.[31] The main objective of such copolymer electrolyte system is to use abundant ester groups of the BA component to capture lithium polysulfides for improving the initial discharge capacity, cycle stability and rate performance of the assembled battery. However, the PIL-based copolymer chains may exhibit deficient movability due to covalently crosslinked networks. In addition, the self-healing properties and the contribution of ester groups to ion conduction were not discussed on the above copolymer electrolyte system.

In this work, a novel PIL-based copolymer electrolyte containing ester groups by copolymerizing imidazolium monomers with butyl acrylate (BA) is prepared. The overall fabrication process is schematically illustrated in Scheme 1. Considering the interaction between main chains of polymer and counter-ions in the PIL-based system,[32] the electrolytes with different counter-anions such as Cl$^-$ and TFSI$^-$ are also synthesized by an ion-exchange reaction at the same time. The **PIL-BA** electrolyte membranes with different counteranions (Fig. S1†) can be easily fabricated by using a simple solvent-casting method using the ethanol solutions of prepared **PIL-BA** copolymers (Fig. S2†). Combining different counteranions and BA will improve the movement of the polymer chains. As a result, compared with PIL homopolymer electrolytes, the PIL-based copolymer electrolytes exhibit high ionic conductivity, excellent mechanical properties and good self-healable capability. It is hoped that the as-prepared PIL copolymer electrolytes could offer new insight into the development of the advanced high-safe polymer electrolytes.

Results and discussion

Firstly, FTIR, ^{1}H NMR and ^{13}C NMR spectra were used to gain insight into the interactions between the counter-ions and main chains of **PIL-BA** copolymer, as shown in Fig. 1. Fig. 1a depicted the FTIR spectra of PIL homopolymers and **PIL-BA** copolymers containing Cl$^-$ or TFSI$^-$ as counter-ions. In the spectrum of **PIL-BA TFSI**, the five characteristic bands attributed to the polymer backbone are observed, assigned to three stretching vibrations of the imidazole ring (3114 cm^{-1}, 1622 cm^{-1}, and 1275 cm^{-1}),[33] a C=O stretching vibration of ester group (1732 cm^{-1}), and a C–O–C stretching vibration of ester group (1111 cm^{-1}); the characteristic bands derived from the TFSI$^-$ anion, such as an SO_2 antisymmetric bending (1354 cm^{-1}), a CF_3 antisymmetric bending (1190 cm^{-1}) and an antisymmetric stretching vibration of the –SO_2–N–SO_2– group (1059 cm^{-1}), have also been detected. Compared with the **PIL-BA TFSI**, the characteristic bands derived from both ester group and imidazole ring of **PIL-BA Cl** were significantly shifted, seen Table S1,† indicating that there was an obvious change of the interaction between ester group or imidazole ring on polymer backbone and counter-ions in the **PIL-BA** copolymer systems. In addition, by comparing with the data of **PIL TFSI**, the characteristic peak of –SO_2–N–SO_2– was blue-shifted from 1055 cm^{-1} to 1059 cm^{-1} and the characteristic peak of CF_3 was blue-shifted from 1198 cm^{-1} to 1190 cm^{-1} in the **PIL-BA TFSI**, indicating that there was a electrostatic interaction (ion–dipole bond) between the electronegative N or F atoms of TFSI$^-$ and ester groups existed in the **PIL-BA TFIS**. Furthermore, the intensity of interaction between polymer backbone and different counterions (TFSI$^-$ or Cl$^-$) can be reflected in the corresponding ^{1}H NMR (Fig. 1b) and ^{13}C NMR spectra (Fig. 1c). The change of chemical shift "g" can be clearly observed in Fig. 1b, which corresponds to the proton in the imidazole ring of the **PIL-BA** main chain.[32] Compared with **PIL-BA Cl**, the proton peak of **PIL-BA TFSI** shifted to the higher field position, from 9.40 ppm to 9.17 ppm, which indicates that the ionic bond interaction between counterions and the positive imidazole ring was weaker after replacing the Cl$^-$ with TFSI$^-$. Moreover, ^{13}C NMR results (Fig. 1c) show that the characteristic peak of C=O derived from BA shifted from 174.22 ppm to 174.08 ppm, further confirming that adding TFSI$^-$ can decrease the interaction intensity between ester group and counterions. Therefore, **PIL-BA** copolymers with TFSI$^-$ counterions have weaker interaction through ionic bonding and ion–dipole bonding, as shown in Fig. 1d. Those results reflected that the larger counter ions (TFSI$^-$) associated less and looser,

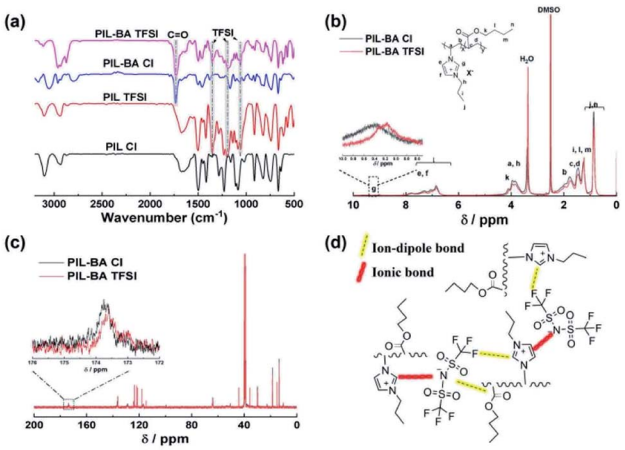

Fig. 1 Confirmation of internal interactions in the **PIL-BA** copolymers. (a) FTIR spectra of the PIL homopolymer and **PIL-BA** copolymer paired with Cl$^-$ or TFSI$^-$. (b) and (c) show the ^{1}H NMR and ^{13}C NMR spectra of the **PIL-BA Cl** and **PIL-BA TFSI**, respectively. (d) The illustration of internal interaction in the **PIL-BA TFSI** system. The yellow dotted line represents ion–dipole bond, the red dotted line represent ionic bond.

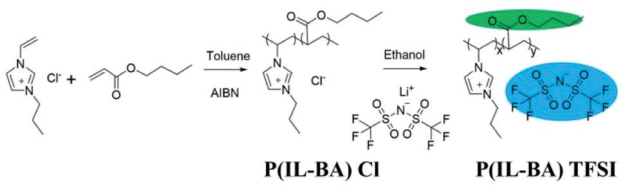

Scheme 1 Schematic illustration of the synthesis of the **PIL-BA** copolymers containing different counter-ions (Cl$^-$ or TFSI$^-$).

benefiting for the decrease of physical cross-links between polymer chains which would cause a decrease in glass-transition temperature (T_g).[15]

Furthermore, the micro-morphology and element analysis of **PIL-BA** based copolymer films with different counter ions can be confirmed by using the SEM-EDS mapping technique, as shown in Fig. 2. It can be seen clearly that the copolymer films are clean and flat without any holes neither for **PIL-BA Cl** nor for **PIL-BA TFSI**. EDS mapping images show that the main elements of **PIL-BA Cl** film (Fig. 2a) are C, O and Cl and those elements are uniformly distributed on the entire material. The results of element analysis of **PIL-BA TFSI** (Fig. 2b) are roughly similar to **PIL-BA Cl**, except that **PIL-BA TFSI** contains the elements of F and S instead of Cl due to the change of counter ions to $TFSI^-$.

To investigate the mobility of polymer chains in **PIL-BA** copolymer based electrolytes, DSC measurements of electrolytes with different counterions were conducted (Fig. 3). **PIL Cl** homopolymer possessed a high T_g of 163 °C, thereby its film was very fragile (see Fig. S2†). After exchanging Cl^- to $TFSI^-$, T_g value of homopolymer PIL based electrolyte was decreased to 153 °C. Such pronounced decrease in T_g is mainly caused by the increase of the fractional free volume originated from the larger counter ions ($TFSI^-$), which is similar to those reported in literature.[32] Furthermore, compared with the homopolymer-based electrolytes, **PIL-BA** copolymer based electrolytes (**PIL-BA Cl** and **PIL-BA TFSI**) have very lower T_g values, and the sample containing $TFSI^-$ has the lowest value of T_g (35.7 °C). It was noting that both of **PIL-BA** copolymers had a similar powder X-ray diffraction pattern (see Fig. S3†), indicating that the exchanging of anions did not change the amorphous structure of PIL which benefited to the movement of chains. It was demonstrated that both the structural units of BA introduced into PIL main chains and using larger counterions could significantly improve the movement of polymer chains. The synergistic effects can further enhance the motility of chains. Combining the DSC results with structural characterization

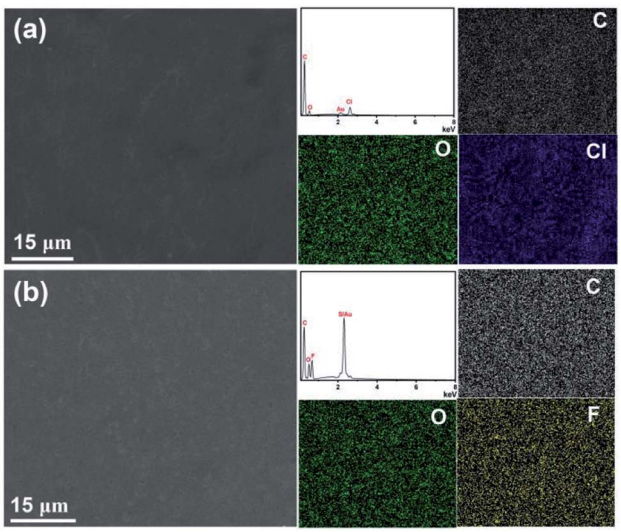

Fig. 2 EDS mapping images of PIL-BA Cl (a) and PIL-BA TFSI (b).

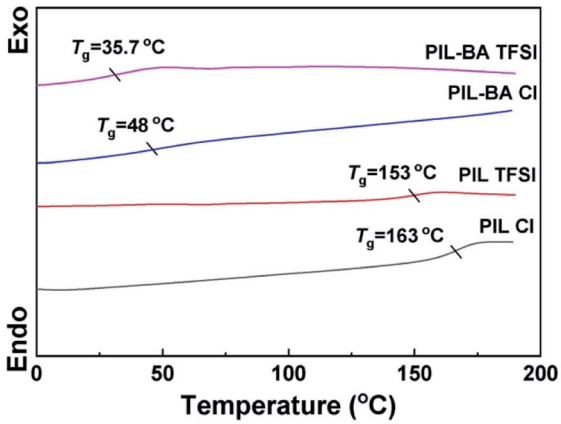

Fig. 3 DSC curves of PIL-BA copolymer based electrolytes with different counter-ions.

(Fig. 1), it inferred that the introduction of larger counter ions ($TFSI^-$) and flexible segment with BA was beneficial to weaken physical cross-links between molecular chains which caused a decrease in T_g.

Before exploring the effect of the different BA content on ion conductive, the molar ratios of ionic liquid monomer and BA incorporated into the copolymers were measured by ^{1}H NMR spectra analyses (Fig. S4†). The results are coincident with the initial feed ratios. Moreover, the molecular weights (M_w) and the polydispersity index (PI) of the **PIL-BA TFSI** based copolymers were tested by gel permeation chromatography (GPC). The GPC analysis shows that the M_w of the polymers with $TFSI^-$ counterions are revealed in the range of 14 000–25 000 and the polydispersity index (PI) of the copolymers are in the range between 1.8 and 2.2 (Table S2†). It is noting that the ion exchange of Cl^- with $TFSI^-$ does not obviously affect the M_w of the copolymer at the same molar ratio. The room temperature ionic conductivities (σ_s) of **PIL-BA** copolymer based electrolytes with different feed molar fractions of BA monomers were studied by EIS measurement (Fig. 4). As shown in Fig. 4a, in the **PIL-BA Cl** systems, the σ significantly increased with the molar fraction of BA and reached 1.57 ± 0.31 mS cm^{-1} at 50 mol% BA (denoted as **PIL-BA$_{50}$ Cl**), which was 6.5 times higher than that of **PIL Cl** without BA (0.24 ± 0.03 mS cm^{-1}). The room temperature σ_s of **PIL-BA TFSI** systems showed same change tendency (see Fig. 4b). It is noted that the σ values of samples

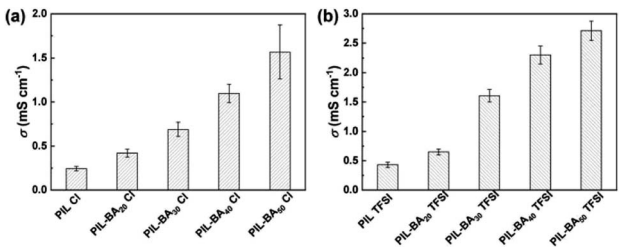

Fig. 4 Ionic conductivities (σ_s) of PIL-BA Cl (a) and PIL-BA TFSI (b) copolymer based electrolytes with various feed molar fraction of BA at room temperature.

containing $TFSI^-$ were higher than that of the electrolytes containing Cl^- at the same molar fraction of BA. As a result, a maximum σ value of 2.71 ± 0.17 mS cm^{-1} was found at **PIL-BA$_{50}$ TFSI**. This phenomenon could be explained by two factors: on the one hand, the larger counterions of $TFSI^-$ can weaken the physical cross-link of main chains, leading to the increase of the chain movement which caused to improve the ion transport; on the other hand, the mobility of polymer chains was further improved by introducing BA units into PIL backbones. In addition, the **PIL-BA** copolymer electrolytes possessed high thermostability that their initial decomposition temperatures were approximately 200 °C (see Fig. S5†). Moreover, the **PIL-BA** copolymer electrolytes were treated at different pH conditions to examine the chemical stability (see Fig. S6†). Although relative intensity of the groups (such as C=O) of the copolymers were decreased under extreme pH conditions (pH = 1 and pH = 11), no characteristic peaks of the copolymers disappeared, indicating that the **PIL-BA** copolymers have excellent stability and can adapt to a variety of pH environments.

Furthermore, the ionic conductivity–temperature plots of the homopolymer **PIL** and copolymer **PIL-BA** based electrolytes paired with different counterions were conducted in Fig. 5. Fig. 5a shows the temperature-dependent impedance curves of **PIL-BA$_{50}$ TFSI** electrolyte from 25 °C to 70 °C. The bulk resistance of the electrolyte were decreased markedly with increasing the temperature, thereby the related σ_s were enhanced. The $\log(\sigma T) \sim 1000/T$ curves was shown in Fig. 5b and corresponding activation energy (E_a) were summarized in Table S2.† The ionic conductivity–temperature curves of the **PIL-BA** based electrolytes were reasonably fitted by the Arrhenius behavior. The E_a values of **PIL Cl** and **PIL TFSI** electrolytes are 13.51 kJ mol^{-1} and 11.58 kJ mol^{-1} respectively. The E_a values of **PIL-BA** copolymer based electrolytes were obviously lower than that of the homopolymer PIL based electrolytes, and **PIL-BA$_{50}$ TFSI** electrolyte has the lowest E_a of 8.68 kJ mol^{-1}. The lower E_a value of **PIL-BA$_{50}$ TFSI** electrolyte indicates that the movement of ions is less affected by temperature changes, also revealing that the ions of system can be transported easier. Therefore, a fast ion transport channel was formed in the **PIL-BA$_{50}$ TFSI** system by decreasing T_g of the polymer.

Because of the superior flexibility of the polymer chains and the weak electrostatic interactions between $TFSI^-$ counterions and polymer backbones in the **PIL-BA$_{50}$ TFSI** system, the **PIL-BA$_{50}$ TFSI** membranes exhibit self-healing ability. As shown in

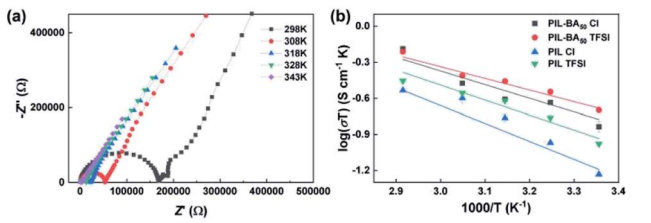

Fig. 5 Influence of the temperature on ionic conductivities of PIL-BA copolymer based electrolytes. AC impedance curves (a) and $\log(\sigma T) \sim 1000/T$ curves (b) at different temperatures.

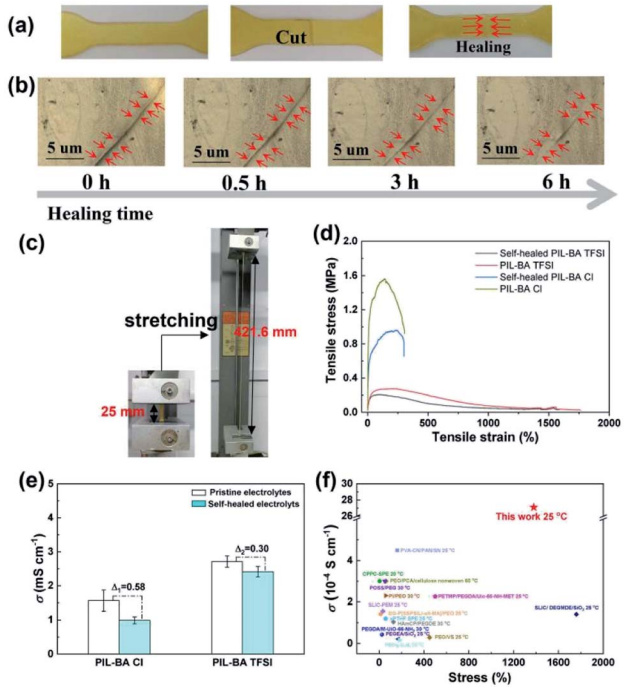

Fig. 6 Photos (a) and optical microscope images (b) of PIL-BA$_{50}$ TFSI electrolytes that were cut into two pieces and then healed at 40 °C for 6 h; (c) photographs showing the high-stretching ability of the healing sample; (d) stress–strain curves of the intact and self-healed PIL-BA$_{50}$ TFSI electrolytes comparing with PIL-BA$_{50}$ Cl; (e) the ionic conductivities of the pristine and self-healed PIL-BA based electrolyte; (f) comparison of the toughness and ionic conductivity of PIL-BA TFSI to other reported polymer electrolytes.

Fig. 6a, the cut **PIL-BA$_{50}$ TFSI** membrane can be self-healed together at 40 °C for 6 h. The optical microscope images in Fig. 6b reveal that the scar is finely healed and gradually disappeared after 6 h at 40 °C. As further evidenced by the tensile tests, the healing sample could withstand stretching to a large extension (from 25 mm to 421.6 mm), shown in Fig. 6c. In addition, the **PIL-BA** polymer electrolyte containing Cl^- counterion was also able to self-heal at 40 °C due to the ionic aggregation behavior.[14,23] Fig. 6d compared the stress–strain curves of the cut **PIL-BA$_{50}$** based samples with different counterions (Cl^- and $TFSI^-$). Those cut polymer electrolytes were self-healed at 40 °C for 6 h. The tensile strength of the cut-healed **PIL-BA$_{50}$ TFSI** and **PIL-BA$_{50}$ Cl** electrolytes can reach ~75% and ~61% of the original values for the intact samples. This observation revealed that the counter ion of $TFSI^-$ increased significantly the healing performance because that $TFSI^-$ ions acting as the plasticizers resulted in a remarkable enhance the mobility of polymer chains, which was in accordance with the DSC results. Moreover, the strain value at break of the **PIL-BA$_{50}$ TFSI** was much higher than that of the **PIL-BA$_{50}$ Cl**, reaching 1762%. Dynamic mechanical analysis (DMA) measurement reveals that the loss modulus (G'') and the storage modulus (G') of the **PIL-BA$_{50}$ TFSI** polymer electrolyte were lower than that of the **PIL-BA$_{50}$ Cl** across the frequency range of 0.1 to 10 Hz (Fig. S7†) due to the decrease in T_g, indicating that

the **PIL-BA$_{50}$ TFSI** polymer electrolyte benefits for the self-healing. Therefore, the obtained **PIL-BA$_{50}$ TFSI** polymer electrolyte exhibited higher recovery of the moduli than that of the **PIL-BA$_{50}$ Cl** upon cutting and self-healing. More importantly, the **PIL-BA$_{50}$ TFSI** polymer electrolyte not only shows better mechanical healed performance as compared to the **PIL-BA$_{50}$ Cl** polymer electrolyte, but also revealed higher healed performance of ionic conductivity than the latter (Fig. 6e). It is also worthwhile noting that **PIL-BA$_{50}$ TFSI** has much higher strain capacity and ionic conductivity than most reported polymer electrolytes (Fig. 6f),[34–47] indicating promising application prospects in all-solid-state electrochemical devices to ensure high security during the long-term cycles.

Experimental

Synthesis of poly(ionic liquid) (PIL) copolymer with different counterions

Poly(ionic liquid)-*co*-butyl acrylate chloride (denoted as **PIL-BA Cl**) was first synthesized *via* radical polymerization of *N*-vinylimidazole-based ionic liquid (VIL) and butyl acrylate (BA) monomers using 2,2-azobis(2-methylpropionitrile) (AIBN, Aladdin agent) as the initiator. The molar ratio of VIL/BA was varied from 5 : 5, 6 : 4, 7 : 3, and 8 : 2. Firstly, the VIL was synthesized by the previously reported methods.[20] Briefly, distilled methylbenzene (8 g), chloropropane (3.14 g, AR, Aladdin agent), and *N*-vinylimidazole (1.88 g, AR, Aladdin agent) were mixed in a 50 mL round-bottomed flask under nitrogen atmosphere, followed by stirring and refluxing the mixture at 50 °C for a period of 12 h. After that, based on the different molar ratios of VIL and BA, a certain weight of BA was added for stirring 10 min at 50 °C. Finally, the initiator of AIBN dissolved into 5 mL methylbenzene was dropwise added into the reaction mixture under vigorous stirring at 65 °C for 48 h. The initiator accounts for 2% of the total monomers. After the polymerization process, the resulting precipitate was filtrated, and repeatedly washed for several times with anhydrous ether, and further purified *via* the Soxhlet extraction and then dried in a vacuum oven at 50 °C. As a contrast, the PIL homopolymers without BA were also synthesized.

Poly(ionic liquid)-*co*-butyl acrylate bis(trifluoromethanesulfonyl)imide (denoted as **PIL-BA TFSI**) was prepared *via* ion exchange metathesis of the above-mentioned **PIL-BA Cl** copolymers. The **PIL-BA** copolymer paired Cl^- (2.0 g) was dissolved in 10 mL deionized water under vigorous stirring to obtain a precursor aqueous solution. Then 7.5 mL aqueous solution of LiTFSI (0.4 M) was slowly added to the precursor aqueous solution dropwise under vigorous stirring for 24 h to exchange the counteranions of the **PIL-BA** copolymers into $TFSI^-$. The resultant precipitate was filtered and thoroughly washed with deionized water to remove the excessive LiTFSI and then dried in a vacuum oven at 50 °C.

The as-prepared PIL copolymers are denoted as PIL-BA$_a$ X, where a represents the feed molar fraction of BA monomers in the copolymer, and X represents the counteranions (X: Cl^-, or $TFSI^-$).

Preparation of PIL-BA copolymer electrolyte membranes

Electrolyte membranes of **PIL-BA** copolymer with different counter-ions were fabricated by the solvent casting method. The as-synthesized **PIL-BA** copolymers (1.00 g) were first dissolved into 10 mL absolute ethyl alcohol and stirred for at least 24 h at room to obtain a precursor aqueous solution (see Fig. S1†). At that same time, the ionic liquid mixture electrolyte consisted of 15 wt% lithium salt (Li-IL) was prepared by dissolving lithium bis(trifluoromethylsulfonyl)imide (99.95%, Sigma-Aldrich) in 1-ethyl-3-methylimidazolium bis(trifluoromethylsulfonyl)imid (99%, Innochem). Then a certain amount of Li-IL was added to the precursor solution dropwise under vigorous stirring for 24 h and subsequently casting onto Teflon substrates (*ca.* 50 mm (L) × 25 mm (D) × 3 mm (T)). The mass fraction of the Li-IL in the copolymer electrolytes were 30 wt%. The cast films were partially allowed to evaporate under ambient conditions in the box filled with argon for 24 h. Finally, the polymer electrolyte membranes were entirely dried under vacuum at 50 °C for 48 h. For testing the ionic conductivity, the membranes were cut into circular samples with a diameter of 16 mm.

Characterizations

Fourier-transform infrared (FT-IR) spectra were conducted on a Bruker Tensor 27 spectrometer in attenuated total reflectance (ATR) mode. For testing the chemical stability of the prepared copolymer electrolytes, the samples were added into different pH values of the aqueous solutions and stirred for 3 days at room temperature. After that, the treated samples were dried and tested by the FT-IR. The NMR spectra of monomers and polymers were recorded on a Bruker-400 MHz spectrometer (399.65 MHz for ^{1}H NMR and 125 MHz for ^{13}C NMR, respectively). The glass transition temperatures (T_gs) of the samples was recorded and analyzed on a differential scanning calorimeter (DSC, TA/Q10). Thermogravimetric analysis (TGA) was performed using a TA Instruments Q50 system from 40 to 600 °C at the heating rate of 10 °C min^{-1} under nitrogen atmosphere. The molecular weight (M_w) and polydispersity index (PI) of the prepared copolymers were measured by gel permeation chromatography (GPC, Agilent PL-GPC50) with the DMF containing 50 mM LiBr as the eluent. The stress–strain test of the electrolyte samples was carried out on a CMT6103 tensile testing machine with a tensile speed of 10 mm min^{-1} at 25 °C. Dynamic mechanical analysis (DMA) measurements were conducted on a TA Instruments DMA 850 with frequency sweeps at 0.1–10 Hz at 25 °C. Healing experiments were tested by gently bringing the cut pieces back into contact at 40 °C. Scanning electron microscopy (SEM) images of the samples were obtained using a Hitachi S-4800 field emission electron microscope equipped with an energy dispersive X-ray fluorescence spectrometer for element analysis.

The ionic conductivities (σ_s) of the electrolytes at different temperatures were calculated using a CHI 660E electrochemical workstation (CH Instruments Inc.) in a coin-cell composed of the electrolyte membranes, two stainless steel as electrodes, using the AC impedance method in the frequency range from 1 MHz to 1 Hz with an amplitude of 5 mV at an open-circuit

potential. The values of σ were calculated using the following equation: $\sigma = L/R_S \times A$, where L, R_S and A were the spacing between two electrodes, the bulk resistance, and the area of the electrode–electrolyte contact, respectively.

Conclusions

In summary, a high ionic conductivity, flexible and self-healing polymer electrolyte was fabricated by copolymerizing imidazolium monomers with butyl acrylate followed with $TFSI^-$ as counteranions. A series of structure characterization proves that an interaction exists between the counter ions and the polymer backbones, which is directly affected by the type of counterions. The introduction of BA units and $TFSI^-$ counteranions gave rise to a low glass transition temperature and free mobility of poly(ionic liquid) (PIL) chains, thus significantly improved the ion conductive (2.71 ± 0.17 mS cm^{-1}) with high toughness (tensile strain of 1762%) and good self-healable capability. The **PIL-BA** copolymer based electrolyte developed in this study may give a new idea to design the molecular structures of polymer electrolytes for secure and stable flexible electronics.

Author contributions

Fu Jie Yang: conceptualization, writing – original draft, writing – reviewing & editing. Qing Feng Liu: formal analysis, visualization, investigation. Xiao Bing Wu: validation, data curation. Yu Yi He: investigation. Xu Gang Shu: project administration, supervision. Jin Huang: writing – reviewing, resources, funding acquisition.

Conflicts of interest

There are no conflicts to declare.

Acknowledgements

This work was financially supported by National Natural Science Foundation of China (Grant No. 52003307), Guangdong Science and Technology Special Fund ("Major Projects + Task List") (Grant No. 2019067), Jieyang Science and Technology Plan Project (Grant No. 2019031), Guangdong Key Laboratory of Radioactive and Rare Resource Utilization (Grant No. 2018B030322009).

References

1 D. P. Dubal, N. R. Chodankar, D.-H. Kim and P. Gomez-Romero, Flexible Solid-State Supercapacitors for Smart and Wearable Electronics, *Chem. Soc. Rev.*, 2018, **47**(6), 2065–2129.

2 W. C. Mai, Q. P. Yu, C. P. Han, F. Y. Kang and B. H. Li, Self-Healing Materials for Energy-Storage Devices, *Adv. Funct. Mater.*, 2020, **30**(24), 1909912.

3 Y. Wang, W. D. Richards, S. P. Ong, L. J. Miara, J. C. Kim, Y. Mo and G. Ceder, Design Principles for Solid-State Lithium Superionic Conductors, *Nat. Mater.*, 2015, **14**, 1026.

4 D. Zhou, D. Shanmukaraj, A. Tkacheva, M. Armand and G. Wang, Polymer Electrolytes for Lithium-Based Batteries: Advances and Prospects, *Chem*, 2019, **5**(9), 2326–2352.

5 Y. H. Jo, S. Li, C. Zuo, Y. Zhang, H. Gan, S. Li, L. Yu, D. He, X. Xie and Z. Xue, Self-Healing Solid Polymer Electrolyte Facilitated by A Dynamic Cross-Linked Polymer Matrix for Lithium-Ion Batteries, *Macromolecules*, 2020, **53**(3), 1024–1032.

6 R. Kato, P. Mirmira, A. Sookezian, G. L. Grocke, S. N. Patel and S. J. Rowan, Ion-Conducting Dynamic Solid Polymer Electrolyte Adhesives, *ACS Macro Lett.*, 2020, **9**(4), 500–506.

7 B. Zhou, C. Zuo, Z. Xiao, X. Zhou, D. He, X. Xie and Z. Xue, Self-Healing Polymer Electrolytes Formed *via* Dual-Networks: A New Strategy for Flexible Lithium Metal Batteries, *Chem.–Eur. J.*, 2018, **24**(72), 19200–19207.

8 Y. Cao, T. G. Morrissey, E. Acome, S. I. Allec, B. M. Wong, C. Keplinger and C. Wang, A Transparent, Self-Healing, Highly Stretchable Ionic Conductor, *Adv. Mater.*, 2017, **29**(10), 1605099.

9 R. Tamate, K. Hashimoto, T. Horii, M. Hirasawa, X. Li, M. Shibayama and M. Watanabe, Self-Healing Micellar Ion Gels Based on Multiple Hydrogen Bonding, *Adv. Mater.*, 2018, **30**(36), 1802792.

10 X. L. Tian, P. Yang, Y. K. Yi, P. Liu, T. Wang, C. Y. Shu, L. Qu, W. Tang, Y. F. Zhang, M. T. Li and B. L. Yang, Self-Healing and High Stretchable Polymer Electrolytes Based on Ionic Bonds with High Conductivity for Lithium Batteries, *J. Power Sources*, 2020, **450**, 227629.

11 Y. X. Lin, H. Y. Zhang, H. Y. Liao, Y. Zhao and K. Li, A Physically Crosslinked, Self-Healing Hydrogel Electrolyte for Nano-Wire PANI Flexible Supercapacitors, *Chem. Eng. J.*, 2019, **367**, 139–148.

12 T. Chen, W. Kong, Z. Zhang, L. Wang, Y. Hu, G. Zhu, R. Chen, L. Ma, W. Yan, Y. Wang, J. Liu and Z. Jin, Ionic Liquid-Immobilized Polymer Gel Electrolyte with Self-Healing Capability, High Ionic Conductivity and Heat Resistance for Dendrite-Free Lithium Metal Batteries, *Nano Energy*, 2018, **54**, 17–25.

13 I. Osada, H. de Vries, B. Scrosati and S. Passerini, Ionic-Liquid-Based Polymer Electrolytes for Battery Applications, *Angew. Chem., Int. Ed.*, 2016, **55**(2), 500–513.

14 J. Cui, Z. Ma, L. Pan, C. H. An, J. Liu, Y. F. Zhou and Y. S. Li, Self-Healable Gradient Copolymers, *Mater. Chem. Front.*, 2019, **3**(3), 464–471.

15 J. Cui, F.-M. Nie, J.-X. Yang, L. Pan, Z. Ma and Y.-S. Li, Novel Imidazolium-based Poly(ionic liquid)s with Different Counterions for Self-healing, *J. Mater. Chem. A*, 2017, **5**(48), 25220–25229.

16 Y. G. Cho, C. Hwang, D. S. Cheong, Y. S. Kim and H. K. Song, Gel/Solid Polymer Electrolytes Characterized by *In Situ* Gelation or Polymerization for Electrochemical Energy Systems, *Adv. Mater.*, 2019, **31**(20), 1804909.

17 Z. Liu, Y. Wang, Y. Ren, G. Jin, C. Zhang, W. Chen and F. Yan, Poly(ionic liquid) Hydrogel-Based Anti-Freezing Ionic Skin for A Soft Robotic Gripper, *Mater. Horiz.*, 2020, **7**(3), 919–927.

18 X. J. Chen, Q. Li, J. Zhao, L. H. Qiu, Y. G. Zhang, B. Q. Sun and F. Yan, Ionic Liquid-Tethered Nanoparticle/Poly(ionic liquid) Electrolytes for Quasi-Solid-State Dye-Sensitized Solar Cells, *J. Power Sources*, 2012, **207**, 216–221.

19 Y. Yu, F. Lu, N. Sun, A. Wu, W. Pan and L. Zheng, Single Lithium-Ion Polymer Electrolytes Based on Poly(ionic liquid)s for Lithium-Ion Batteries, *Soft Matter*, 2018, **14**(30), 6313–6319.

20 F. J. Yang, Y. F. Huang, M. Q. Zhang and W. H. Ruan, Significant Improvement of Ionic Conductivity of High-Graphene Oxide-Loading Ice-Templated Poly (ionic liquid) Nanocomposite Electrolytes, *Polymer*, 2018, **153**, 438–444.

21 H. Zhang, C. Liu, L. Zheng, W. Feng, Z. Zhou and J. Nie, Solid Polymer Electrolyte Comprised of Lithium Salt/Ether Functionalized Ammonium-Based Polymeric Ionic Liquid with Bis(fluorosulfonyl)imide, *Electrochim. Acta*, 2015, **159**, 93–101.

22 F. Fan, W. Y. Wang, A. P. Holt, H. B. Feng, D. Uhrig, X. Y. Lu, T. Hong, Y. Y. Wang, N. G. Kang, J. Mays and A. P. Sokolov, Effect of Molecular Weight on the Ion Transport Mechanism in Polymerized Ionic Liquids, *Macromolecules*, 2016, **49**, 4557–4570.

23 F.-M. Nie, J. Cui, Y.-F. Zhou, L. Pan, Z. Ma and Y.-S. Li, Molecular-Level Tuning toward Aggregation Dynamics of Self-Healing Materials, *Macromolecules*, 2019, **52**(14), 5289–5297.

24 X. E. Wang, H. J. Zhu, G. M. A. Girard, R. Yunis, D. R. MacFarlane, D. Mecerreyes, A. J. Bhattacharyya, P. C. Howlett and M. Forsyth, Preparation and Characterization of Gel Polymer Electrolytes Using Poly(ionic liquids) and High Lithium Salt Concentration Ionic Liquids, *J. Mater. Chem. A*, 2017, **5**, 23844–23852.

25 Y. H. Li, Z. J. Sun, L. Shi, S. Y. Lu, Z. H. Sun, Y. C. Shi, H. Wu, Y. F. Zhang and S. J. Ding, Poly(ionic liquid)-Polyethylene Oxide Semi-Interpenetrating Polymer Network Solid Electrolyte for Safe Lithium Metal Batteries, *Chem. Eng. J.*, 2019, **375**, 121925.

26 J. R. Nykaza, A. M. Savage, Q. Pan, S. Wang, F. L. Beyer, M. H. Tang, C. Y. Li and Y. A. Elabd, Polymerized Ionic Liquid Diblock Copolymer as Solid-State Electrolyte and Separator in Lithium-Ion Battery, *Polymer*, 2016, **101**, 311–318.

27 H. Zhang, C. M. Li, M. Piszcz, E. Coya, T. Rojo, L. M. Rodriguez-Martinez, M. Armand and Z. B. Zhou, Single Lithium-Ion Conducting Solid Polymer Electrolytes: Advances and Perspectives, *Chem. Soc. Rev.*, 2017, **46**(3), 797–815.

28 K. W. Lee, J. W. Chung and S. Y. Kwak, Structurally Enhanced Self-Plasticization of Poly(vinyl chloride) *via* Click Grafting of Hyperbranched Polyglycerol, *Macromol. Rapid Commun.*, 2016, **37**(24), 2045–2051.

29 S. Song, Z. Xing, Z. Cheng, Z. Fu, J. Xu and Z. Fan, Functional Polyethylene with Regularly Distributed Ester Pendants *via* Ring-Opening Metathesis Polymerization of Ester Functionalized Cyclopentene: Synthesis and Characterization, *Polymer*, 2017, **129**, 135–143.

30 P. Guo, H. Zhang, X. Liu and J. Sun, Counteranion-Mediated Intrinsic Healing of Poly(ionic liquid) Copolymers, *ACS Appl. Mater. Interfaces*, 2018, **10**(2), 2105–2113.

31 X. M. Cai, B. W. Cui, B. Ye, W. Q. Wang, J. L. Ding and G. H. Wang, Poly(ionic liquid) Based Quasi-Solid-State Copolymer Electrolytes for Dynamic-reversible Adsorption of Lithium Polysulfides in Lithium-Sulfur Batteries, *ACS Appl. Mater. Interfaces*, 2019, **11**, 38136–38146.

32 J. Cui, F. M. Nie, J. X. Yang, L. Pan, Z. Ma and Y. S. Li, Novel Imidazolium-Based Poly(ionic liquid)s with Different Counterions for Self-Healing, *J. Mater. Chem. A*, 2017, **5**(48), 25220–25229.

33 X. Chen, J. Zhao, J. Zhang, L. Qiu, D. Xu, H. Zhang, X. Han, B. Sun, G. Fu, Y. Zhang and F. Yan, Bis-Imidazolium Based Poly(Ionic Liquid) Electrolytes for Quasi-Solid-State Dye-Sensitized Solar Cells, *J. Mater. Chem.*, 2012, **22**(34), 18018–18024.

34 D. G. Mackanic, X. Z. Yan, Q. H. Zhang, N. Matsuhisa, Z. A. Yu, Y. W. Jiang, T. Manika, J. Lopez, H. P. Yan, K. Liu, X. D. Chen, Y. Cui and Z. A. Bao, Decoupling of Mechanical Properties and Ionic Conductivity in Supramolecular Lithium Ion Conductors, *Nat. Commun.*, 2019, **10**, 5384.

35 Z. Wang, S. Wang, A. Wang, X. Liu, J. Chen, Q. Zeng, L. Zhang, W. Liu and L. Zhang, Covalently Linked Metal-Organic Framework (MOF)-Polymer All-Solid-State Electrolyte Membranes for Room Temperature High Performance Lithium Batteries, *J. Mater. Chem. A*, 2018, **6**, 17227–17234.

36 J. Wan, J. Xie, X. Kong, Z. Liu, K. Liu, F. Shi, A. Pei, H. Chen, W. Chen, J. Chen, X. Zhang, L. Zong, J. Wang, L.-Q. Chen, J. Qin and Y. Cui, Ultrathin, Flexible, Solid Polymer Composite Electrolyte Enabled with Aligned Nanoporous Host for Lithium Batteries, *Nat. Nanotechnol.*, 2019, **14**(7), 705.

37 D. G. Mackanic, W. Michaels, M. Lee, D. W. Feng, J. Lopez, J. Qin, Y. Cui and Z. N. Bao, Crosslinked Poly(tetrahydrofuran) as a Loosely Coordinating Polymer Electrolyte, *Adv. Energy Mater.*, 2018, **8**(25), 1800703.

38 J. Zhang, J. Zhao, L. Yue, Q. Wang, J. Chai, Z. Liu, X. Zhou, H. Li, Y. Guo, G. Cui and L. Chen, Safety-Reinforced Poly(propylene carbonate)-Based All-Solid-State Polymer Electrolyte for Ambient-Temperature Solid Polymer Lithium Batteries, *Adv. Energy Mater.*, 2015, **5**, 1501082.

39 D. Zhou, Y.-B. He, R. Liu, M. Liu, H. Du, B. Li, Q. Cai, Q.-H. Yang and F. Kang, In Situ Synthesis of a Hierarchical All-Solid-State Electrolyte Based on Nitrile Materials for High-Performance Lithium-Ion Batteries, *Adv. Energy Mater.*, 2015, **5**(15), 1500353.

40 C. Zuo, M. Yang, Z. Wang, K. Jiang, S. Li, W. Luo, D. He, C. Liu, X. Xie and Z. Xue, Cyclophosphazene-Based Hybrid Polymer Electrolytes Obtained *via* Epoxy-Amine Reaction for High-Performance All-Solid-State Lithium-Ion Batteries, *J. Mater. Chem. A*, 2019, **7**, 18871–18879.

41 Z. Sun, Y. Li, S. Zhang, L. Shi, H. Wu, H. Bu and S. Ding, g-C_3N_4 Nanosheets Enhanced Solid Polymer Electrolytes with Excellent Electrochemical Performance, Mechanical

Properties, and Thermal Stability, *J. Mater. Chem. A*, 2019, **7**(18), 11069–11076.

42 C. Q. Niu, J. Liu, G. P. Chen, C. Liu, T. Qian, J. J. Zhang, B. K. Cao, W. Y. Shang, Y. B. Chen, J. L. Han, J. Du and Y. Chen, Anion-Regulated Solid Polymer Electrolyte Enhances the Stable Deposition of Lithium Ion for Lithium Metal Batteries, *J. Power Sources*, 2019, **417**, 70–75.

43 G. Luo, B. Yuan, T. Guan, F. Cheng, W. Zhang and J. Chen, Synthesis of Single Lithium-Ion Conducting Polymer Electrolyte Membrane for Solid-State Lithium Metal Batteries, *ACS Appl. Energy Mater.*, 2019, **2**(5), 3028–3034.

44 C. Cao, Y. Li, S. Chen, C. Peng, Z. Li, L. Tang, Y. Feng and W. Feng, Electrolyte-Solvent-Modified Alternating Copolymer as a Single-Ion Solid Polymer Electrolyte for High-Performance Lithium Metal Batteries, *ACS Appl. Mater. Interfaces*, 2019, **11**(39), 35683–35692.

45 Z. Y. Huang, Q. W. Pan, D. M. Smith and C. Y. Li, Plasticized Hybrid Network Solid Polymer Electrolytes for Lithium-Metal Batteries, *Adv. Mater. Interfaces*, 2018, **6**, 1801445.

46 H. Wang, Q. Wang, X. Cao, Y. He, K. Wu, J. Yang, H. Zhou, W. Liu and X. Sun, Thiol-Branched Solid Polymer Electrolyte Featuring High Strength, Toughness, and Lithium Ionic Conductivity for Lithium-Metal Batteries, *Adv. Mater.*, 2020, **32**, 2001259.

47 J. J. Zhang, L. P. Yue, P. Hu, Z. H. Liu, B. S. Qin, B. Zhang, Q. F. Wang, G. L. Ding, C. J. Zhang, X. H. Zhou, J. H. Yao, G. L. Cui and L. Q. Chen, Taichi-Inspired Rigid-Flexible Coupling Cellulose-Supported Solid Polymer Electrolyte for High-Performance Lithium Batteries, *Sci. Rep.*, 2014, **4**, 6272.